Numerical analysis of the behaviour of mechanically stabilized earth walls reinforced with different types of strips

Abdelkader Abdelouhab [a,*], Daniel Dias [a], Nicolas Freitag [b]

[a] Inst. Nat. Sc. Appl. Lyon, Laboratory of Civil and Environmental Engineering, LGCIE, 20 av. A. Einstein, F-69621 Villeurbanne Cedex, France
[b] Terre Armée Internationale, 1 bis, rue du Petit Clamart, 78140 Vélizy-Villacoublay, France

ABSTRACT

A mechanically stabilized earth (MSE) wall behaves as a flexible coherent block able to sustain significant loading and deformation due to the interaction between the backfill material and the reinforcement elements. The internal behaviour of a reinforced soil mass depends on a number of factors, including the soil, the reinforcement and the soil/structure interaction and represents a complex interaction sol/structure problem. The use of parameters determined from experimental studies should allow more accurate modelling of the behaviour of the MSE structures.

In this article, a reference MSE wall is modelled from two points of view: serviceability limit state "SLS" and ultimate limit state "ULS". The construction of the wall is simulated in several stages and the soil/interface parameters are back analysed from pullout tests. An extensive parametric study is set up and permits to highlight the influence of the soil, the reinforcement and the soil/structure parameters. The behaviour of MSE walls with several geosynthetic straps is compared with the metallic one. Several constitutive models with an increasing complexity have been used and compared.

The results obtained from stress-deformation analyses are presented and compared. The use of geosynthetic straps induces more deformation of the wall but a higher safety factor. To design theses walls the important parameters are: the soil friction, the cohesion, the interface shear stiffness and the strip elastic modulus.

It is shown that for wall construction that involves static loading conditions, the modified Duncan–Chang model is a good compromise but induces slightly lower strip tensile forces due to the fact that it do not take into account of dilatancy before failure.

© 2010 Elsevier Ltd. All rights reserved.

1. Introduction

The MSE wall is a composite material formed by the combination of soil and metallic or synthetic strips able to sustain significant tensile loads. The reinforcing strips give to the soil mass an anisotropic cohesion in the direction perpendicular to the reinforcement (Schlosser and Elias, 1978). The presence of the strips improves the overall mechanical properties of the soil. The design methods used in these structures are based on the internal and external stability analysis using limit equilibrium methods. For the internal stability, the common method is based on the verification of the strip long-term tensile force and the adherence or bond capacity at the soil/strip interface (AASHTO, 2002; NF P 94-270, 2009; BS 8006, 1995). Although sometimes described as excessively conservative for the synthetic reinforcement (Elias et al., 2001; Koerner and Soong, 2001; Allen et al., 2002; Bathurst et al., 2005), this straightforward design methodology allows verifying the structure stability (Yoo and Jung, 2006; Quang et al., 2008) but does not make it possible to determine the deformation state of the structure.

In order to make new steps in the optimization of the design method, it is essential to understand the behaviour of such structures. Several studies, experimental, theoretical or numerical, have been carried out with this objective.

The experimental studies present the inconvenience that they are expensive and time-consuming. They are commonly focused on the definition of the parameters of new elements such as new reinforcement types, new facing panels or the interface between soil and new reinforcement types (e.g., Park and Tan, 2005; Yoo and Kim, 2008; Won and Kim, 2007).

The theoretical studies are mainly dedicated to the definition of new anchorage models taking into account the actual behaviour of the new reinforcement (e.g., Leshchinsky, 2009; Ling et al., 2005;

* Corresponding author.
E-mail addresses: abdelkader.abdelouhab@insa-lyon.fr (A. Abdelouhab), daniel.dias@insa-lyon.fr (D. Dias), nicolas.freitag@terre-armee.com (N. Freitag).

Notation

A	Deviatoric slope in CJS2 model
CJS2	Simplified version of the CJS model developed by Cambou and Jafari (1987) for cohesionless soils
D&C	Duncan and Chang hyperbolic constitutive model
E	Young modulus
Fs	Factor of safety
Fsr	Factor of safety in the reference model
GS 50	Geosynthetic reinforcement strips (GeoStrap 50) used in MSE Walls
GSHA	New geosynthetic strips (GeoStrap High Adherence) used in MSE Walls
G	Shear modulus (MPa)
G_0	Material parameters for the reference pressure in CJS2 model
I_1	First stress invariant in CJS2 model
J	Geosynthetic elongation modulus (kN/m)
K	Bulk modulus (MPa)
K_y	Young's modulus parameter of Duncan and Chang
K_B	Bulk's modulus parameters of Duncan and Chang
K_0^p	Plastic bulk modulus for the reference pressure in CJS2 model (MPa)
K_0	Material parameters for the reference pressure in CJS2 model
L	Strip length (m)
MC	Elastic linear perfectly plastic soil constitutive model with the Mohr−Coulomb plasticity criterion
MSE	Mechanically Stabilized Earth
Pa	Atmospheric pressure used for normalization of the stress input
P'	Average effective confining pressure
Q	Hardening variable determined by the isotropic hardening mechanism
R_f	Failure Ratio coefficient which represents the failure vicinity in D&C model
R_c	Characteristic surface of CJS2 model
R_m	Size of the failure surface related to the friction angle in CJS2 model
SLS	Serviceability Limit State
T_{max}	Maximum shear force (tensile force) on the strip
ULS	Ultimate Limit State
lUl	Maximal displacement of the reinforced backfill
U_x	Maximal horizontal displacement of the reinforced backfill
U_y	Maximal vertical displacement of the reinforced backfill
U_r	Deformation in the reference model
U^*	Relative soil/strip displacement at the total mobilisation of the strip in pullout tests for one meter width of wall
c	Soil cohesion (kPa)
f	Apparent friction coefficient at the soil/strip interface ($f = \tau/\sigma_v$)
f_d	Yield function of the deviatoric mechanism
f^*	Maximum apparent friction coefficient at the soil/strip interface ($f^* = \tau_{max}/\sigma_v$)
h	Function of the Lode angle
k_b	Shear stiffness at the soil/strip interface
n	Material parameters for the reference pressure Pa in CJS2 model
n_B	Volumetric parameter in Duncan and Chang model
n_Y	Young modulus parameter in Duncan and Chang model
s_{II}	Deviatoric stress tensor second invariant
β	Dilatancy slope in CJS2 model
γ	Parameter of CJS2 model
τ	Shear stresses exerted by reinforcements (kN/m^2)
τ_{max}	Maximum shear stresses exerted by reinforcements (kN/m^2)
ε	Locale strip deformation
φ	Soil friction angle (°)
θ	Lode angle in CJS2 model
ψ	Dilatancy angle
ν	Poisson's ratio
σ_{v0}	Initial vertical stress applied on the strips
$\Delta\sigma_v$	Increase of the vertical stress σ_{v0} due to the phenomenon of constrained dilatancy
ΔFs	Difference between Fsr and the Fs obtained from the most influential value
ΔU	Difference between Ur and the lUl obtained from the most influential value

Koerner and Soong, 2001; Yoo and Jung, 2006; Sieira et al., 2009; Khedkar and Mandal, 2009; Su et al., 2008; Abdelouhab et al., 2009).

In the numerical studies, two and three-dimensional methods based on finite elements or finite differences (Ho and Rowe, 1994; Hatami and Bathurst, 2006; Skinner and Rowe, 2005; Al Hattamleh and Muhunthan, 2006; Bergado and Teerawattanasuk, 2008) allow the authors to analyse the deformation and the influence of several parameters in some types of reinforced soil walls. Huang et al. (2009) and Ling and Liu (2009) have studied different soil constitutive models and their influence on results. They conclude that the modified Duncan−Chang model is a good compromise between prediction accuracy and availability of parameters from conventional triaxial compression testing. However, interface parameters used in these studies (friction and shear stiffness at soil/reinforcement interface) are considered constant from the surface to the base of the wall.

In this article, a two-dimensional numerical analysis of an MSE wall is carried out using the explicit finite difference software FLAC 2D (Itasca Consulting Group, 2006).

In the first part, this paper presents a reference wall reinforced by synthetic reinforcements. Differences and similarities between geosynthetic reinforcements and metallic reinforcements are

highlighted. The soil/interface parameters are back analysed from pullout tests (Abdelouhab et al., 2009).

In the second part, the influence of several parameters (soil/strip interface, strips and soil) on the behaviour of the MSE wall is shown. To satisfy the serviceability limit state criteria, a structure must remain functional for its intended use subject to routine loading, and as such the structure must not cause occupant discomfort under routine conditions. To satisfy the ultimate limit state, the structure must not collapse when subjected to the peak design load for which it was designed. The criteria used in this study are deformation (serviceability limit state "SLS") and global stability (ultimate limit state "ULS").

2. Two-dimensional modelling

A 6 m high reference MSE Wall is modelled using the finite difference numerical analysis program *Fast Lagrangian Analysis of Continua* FLAC 2D (Itasca Consulting Group, 2006). This case is an academic one using realistic geometrical and geotechnical parameters.

This numerical program FLAC 2D allows the resolution of stress−strain problems in a continuous area. At every point of the
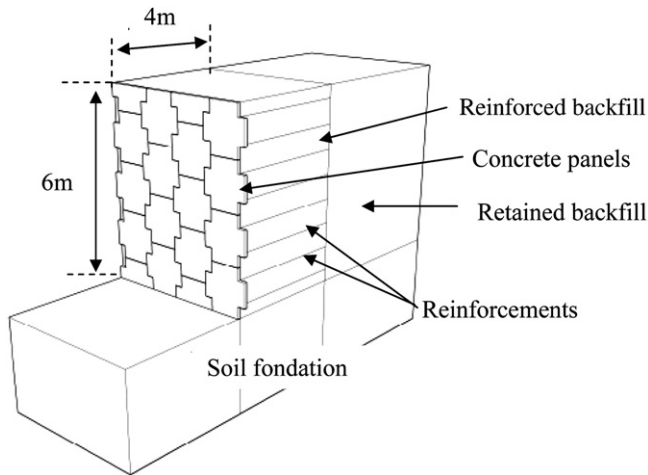
Fig. 1. Geometry of the modelled wall.

Table 1
Geomechanical characteristics.

	Reinforced backfill	Retained backfill	Foundation soil
Constitutive model	Mohr Coulomb	Mohr Coulomb	Elastic linear
Young modulus (MPa)	50	30	200
Poisson's ratio	0.3	0.3	0.25
Unit weight (kg/m³)	1580	1800	2000
Friction angle (°)	36	30	–
Dilatancy angle (°)	6	0	–
Cohesion (kPa)	0	0	–

range, the stress and strain tensor is known, which allows viewing the events in. The program is based on the finite difference method: the variables are known in discrete locations in space and it is not necessary to store a global stiffness matrix.

2.1. Presentation of the numerical model

The simulated 6 m high wall is made of 4 superimposed panels and reinforced by 8 levels of 4 m long reinforcement layers (Fig. 1).

The cruciform geometry of the panels (Fig. 2a), leads to a complex geometry of the wall. This three-dimensional geometry and staggered layout are simplified into a two-dimensional model using some simplifications. Two panels are considered as the width of calculation, with 4 connecting points for strips at each level over 3 m course. The panels are modelled like rectangular plates of 1.5 m by 1.5 m (Fig. 2b).

The simplification of the geometry makes it possible to use a two-dimensional model with continuous reinforcements. The characteristics of these reinforcements are calculated as being the ratio of characteristics for the width of considered ground (Fig. 2c).

For the boundary conditions, horizontal and vertical displacements are blocked at the bottom of the model and horizontal displacements are blocked on the lateral limits.

In order to model with accuracy the actual construction stages, the reinforced backfill and the retained backfill are modelled by layers of 0.375 m height in 8 stages:

- Stage 1: set up of the first concrete panel, the first and the second soil layer and installation of the first strip between the

two layers of the reinforced backfill (equilibrium under self-weight).
- Stage 2: placement of the third and the fourth layer, installation of the second strip between the two layers of the reinforced backfill (equilibrium under self-weight).
- Stage 3: set up of the second beam, the fifth and sixth layer and installation of the third strip between the two layers of the reinforced backfill.
- These phases are repeated up to 6 m height.

2.2. Geomechanical parameters of the reference case

The reference case is an academic one but with geomechanical parameters of actual soils back analysed from triaxial tests. The soil/reinforcement interface parameters are back analysed from pullout tests. These reference parameters are described below.

In none of the calculations the incremental lateral movement of the facing during construction has been taken into account. The effect of soil compaction is not considered in the reference case. It is investigated in the following study.

2.2.1. Soils

The model is constituted of three different soils (Fig. 1) characteristics of which are reported in Table 1:

- Reinforced backfill: simulated by uniform fine dense sand known as Hostun RF sand (Gay, 2000; Flavigny et al., 1990).
- Retained backfill.
- Foundation soil.

The constitutive model to simulate the behaviour of the reinforced backfill and the retained backfill is a linear elastic, perfectly plastic model with the Mohr–Coulomb's failure criterion (named MC in this study).

This constitutive model is characterised by five parameters: elastic parameters (*E*: Young modulus, *ν*: Poisson's ratio) and plastic
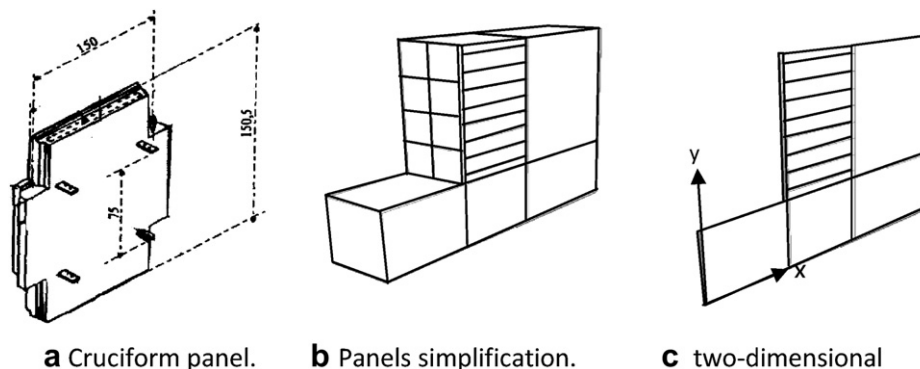

a Cruciform panel. **b** Panels simplification. **c** two-dimensional

Fig. 2. Representation of a three-dimensional structure by a two-dimensional model.

parameters (φ: friction angle, c: cohesion, and ψ: dilatancy angle). The parameters of this constitutive model were defined for the reinforced soil by calibration on triaxial tests carried out under confinement of 30 kPa, 60 kPa and 90 kPa (Fig. 3a and b).

For the foundation soil, a linear elastic constitutive model is used. This model is characterised by two elastic parameters (E: Young modulus and ν: Poisson's ratio).

2.2.2. Concrete panels

The panels are modelled using *Beam* elements. They are used to represent structural elements and take into account effects of bending resistance and limited bending moments. Tensile and compressive yield strength limits can also be specified (Table 2).

In order to reproduce the flexibility of the actual wall facing, the beams were connected by pins. In the actual structure, wall panel spacers made of ribbed elastomeric pads, are inserted between panels to help provide the proper spacing. Proper spacing keeps the panels from having contact points and spalling of the concrete. The elastomeric pads are taken into account in numerical modelling by reducing artificially the beam section but keeping its actual inertia moment.

2.2.3. Interaction between concrete panels and soil

Interface elements were attached on one side of beam elements in order to simulate the frictional interaction between the smooth concrete facing panels and the backfilling soil (Table 3). The normal and the shear stiffness are calculated using the FLAC recommendations and the friction angle is estimated to be equal to 2/3 of the soil friction angle.

2.2.4. Reinforcements

The reinforcement simulated in the reference calculation is a synthetic strip (GS 50) containing high-tenacity polyester yarns protected by polyethylene sheath. Its properties are presented in Table 4, column 1.

However, as the behaviour of MSE Wall depends mainly on the reinforcement type, two other strip types were studied:

- High Adherence Metallic strips: commonly used in the reinforced soil structures (Table 4, column 2).
- New High Adherence synthetic strips (GS HA): this product has been developed during our experimental research works. As with the GS 50, this strip is made of high-tenacity polyester yarns protected by polyethylene sheath but manufactured under a new geometric shape. It has the same in-air axial

Table 2
Concrete panels characteristics.

Parameter	
Constitutive model	Elastic linear
Young modulus (MPa)	15,000
Poisson's ratio	0.2
Density (kg/m^3)	2500

stiffness. It offers by its lateral teeth, a higher adherence with the soil (Table 4, column 3).

The reinforcements are modelled using *Strip* elements, specifically designed to simulate the behaviour of thin, flat and discrete reinforcing strips. The *Strip* element can yield in compression and tension. They provide shear resistance but cannot sustain bending moments.

2.2.5. Soil/reinforcement interface parameters

The shear behaviour of the strip/soil interface is defined by a nonlinear shear failure envelope that varies as a function of the confining pressure. The interface parameters are the apparent friction coefficient f^* and the shear stiffness k_b at the soil/strip interface. The friction coefficient at the soil/strip interface f is expressed as:

$$f = \frac{\tau_{max}}{\sigma_{v0} + \Delta\sigma_v} \tag{1}$$

τ_{max} is the maximum shear stresses exerted by reinforcements;

σ_{v0} is the initial vertical stress applied on strips;

$\Delta\sigma_v$ is the increase of vertical stress due to the phenomenon of the constrained dilatancy.

For a compacted granular soil, the soil/inclusion shearing will lead to volumetric dilation that will be constrained by the surrounding soil and causes local increase of the vertical stress. To take into account this three-dimensional phenomenon in the two-dimensional design methods, Schlosser and Elias (1978) defined an apparent friction coefficient f^*:

$$f^* = \frac{\tau_{max}}{\sigma_{v0}} \tag{2}$$

The increase of the friction coefficient due to the constrained dilatancy effect will only be significant at a low vertical stress, but will be negligible when the volume of soil cannot increase under
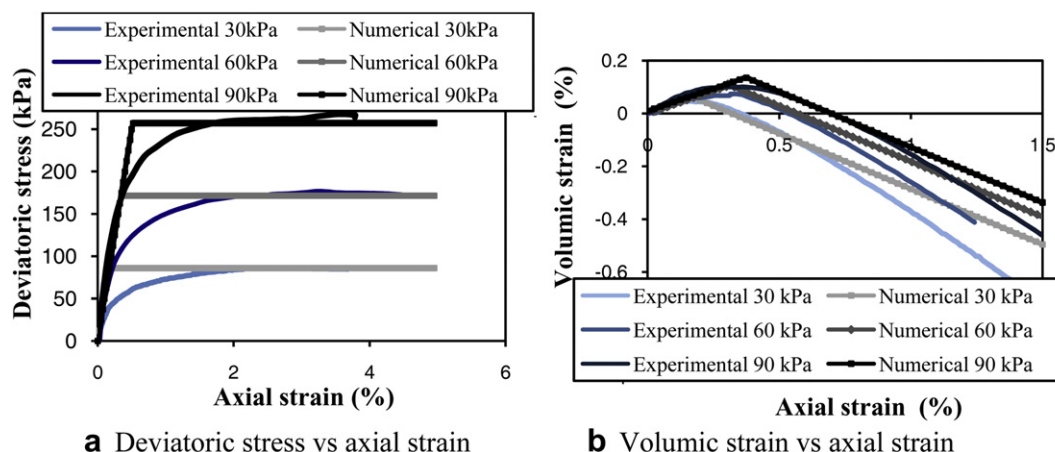

Fig. 3. Calibration of numerical models on triaxial tests.

Table 3
Concrete panel/soil interface characteristics.

Parameter	
Constitutive model	Coulomb sliding
Normal stiffness (MPa)	1000
Shear stiffness (MPa)	1000
Friction angle at panel/soil interface (°)	24

a high vertical stress. This coefficient decreases as the confinement stress increases. It varies between f^*_0 and f^*_1 from the surface of the soil mass to 6 m depth (Fig. 4, (NF P 94 220, 1998)).

The shear stiffness at the soil/strip interface (k_b) is defined as:

$$k_b = \frac{T_{max}/L}{U^*} \qquad (3)$$

T_{max} is the maximum shear force (tensile force) on the strip

L is the strip length

U^* is the relative soil/strip displacement at the total mobilisation of the strip in pullout tests for a wall of 1 m width.

The values of the friction coefficient (f^*) and the shear stiffness (k_b) parameter taken in the numerical model were defined by calibration on laboratory pullout tests. In fact, several tests were carried out in a metallic tank of 2 m^3. They consisted in pulling out a strip of 2 m length anchored at the centre of the tank in uniform dense sand (Abdelouhab et al., 2009). This uniform dense sand is similar to the reinforced soil simulated in the numerical model. The pullout tests (Fig. 5) were modelled numerically and allowed us to define the soil/strip interface parameters to use in the MSE Wall modelling.

The dimensions of the physical model have been kept in the modelling. The mesh was refined around the strip in order to have accurate results.

Several tests with different confinement stresses have been modelled (7 kPa, 22 kPa, 40 kPa and 80 kPa) in order to simulate different depth level. Fig. 6 shows the calibration of the numerical results on the experimental tests carried out under confinement stresses of 8 kPa and 40 kPa. In the reference numerical modelling of MSE Wall, as in standards, an average value of the shear stiffness has been used. However, in order to highlight the influence of the variation of this parameter versus the confinement stresses, as in the actual conditions, a modelling of the MSE Wall was made taking into account different values from the top to the bottom of the wall.

The parameters used in the reference numerical modelling are presented on Table 5.
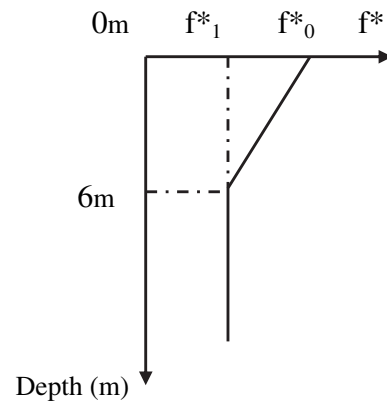

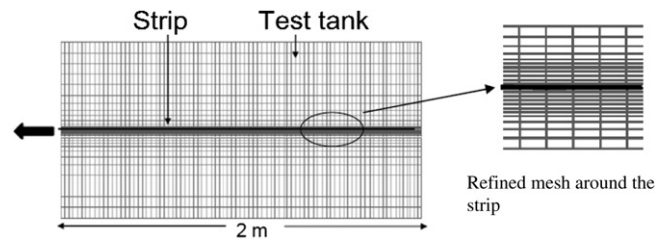**Fig. 4.** Variation of the apparent friction coefficient in the soil mass.

Fig. 5. Numerical modelling of pullout tests.

2.3. Comparison criteria

Two criteria are used to study the MSE Walls behaviour: a deformation criterion (serviceability limit state "SLS") and a stability criterion (ultimate limit state "ULS").

The deformation criterion of the wall is calculated using the norm of the maximal displacement $|U|$ of the reinforced backfill:

$$|U| = \sqrt{\left(U_x^2 + U_y^2\right)} \qquad (4)$$

Analysis of the walls stability has been carried out by calculation of the factor of safety (Fs). This factor is calculated by the $c-\varphi$ reduction process. In this approach the strength parameters of the reinforced backfill and the retained backfill (friction and cohesion) are successively reduced until failure of the structure occurs. The factor of safety is then given by:
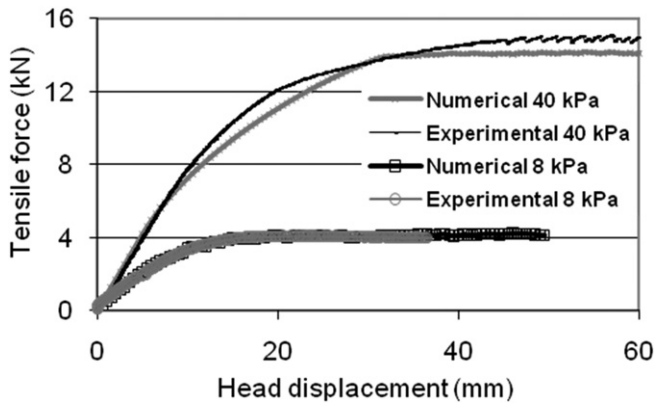
Table 4
Reinforcements characteristics.

Reinforcements	GS 50	Metallic	GS HA
Constitutive model	Elastic linear	Elastic linear	Elastic linear
Elastic modulus of the strip (GPa)	2.5	210	2.5
Width (m)	0.1	0.05	0.1
Thickness (mm)	3	4	3
Strip tensile yield-force limit (KN)	100	100	70
Strip compressive yield–force limit (N)	0.0	100	0.0
Tensile failure strain limit of strip (%)	12	10	12

Fig. 6. Calibration of the numerical results on the experimental pullout tests.

Table 5
Soil/reinforcements interface characteristics.

Parameter	GS 50	Metallic	GS HA
Constitutive model	Coulomb sliding	Coulomb sliding	Coulomb sliding
Initial apparent friction coefficient at the soil/strip interface "f^*_0"	1.2	1.5	2.5
Minimum apparent friction coefficient at the soil/strip interface "f^*_1"	0.6	0.727	1
Shear stiffness at the soil strip interface k_b (MN/m²/m)	0.22	1.6	0.25

$$Fs = \frac{\text{initial strength}}{\text{strength at failure}} \qquad (5)$$

This stability criterion offers a measurement of the mixed stability of the structure. It does not represent the levels of internal stability as required by the current standard (long-term breaking strength and adherence of each reinforcement layer).

2.4. Results (reference case)

The maximum displacement calculated on the MSE Wall using reference parameters with synthetic strips (G50) is equal to 78 mm (Table 6). This high value is due to the fact that the synthetic strips present a low stiffness. In a real work, this high horizontal displacement (61 mm) can be corrected at each construction step. A small variation of the concrete panel batter (about 2% on the height

Table 6
Reference calculation results on synthetic strips.

SLS			ULS
$|U|$ (mm)	$|U_x|$ (mm)	$|U_y|$ (mm)	Fs
78	61	53	1.51

Table 7
Influence of the soil parameters.

Parameter	Varied between		Most influential value	$I\Delta Fsl/Fsr$ (%)	$I\Delta Ul/Ur$ (%)
	Min	Max			
Young modulus (MPa)	20	100	100	2	3
Poisson's ratio	0.25	0.35	0.35	2	3
Friction angle (°)	30	40	30	6	45
Dilatancy (°)	2	36	36	2	18
Cohesion (kPa)	0	40	20 and 40	7	84

Fsr, safety factor in the reference model; U_r, deformation in the reference model; ΔFs, difference between the Fsr and the Fs obtained by the most influential value; ΔU, difference between the Ur and the U obtained by the most influential value.

of the panel) is permitted. This small variation allows to reduce the horizontal deformation of the wall facing.

At the base of the wall, the settlement is equal to 5 mm. The maximum vertical displacement of the wall is equal to 53 mm. So it means that the settlement at the base of the wall is ten times less than the maximum settlement of the wall.

Concerning the stability of the wall, the Fs calculation shows a high stability for the MSE Wall.

At failure, one can observe a sliding at the vicinity of the base, accompanied with a rupture of adherence of the bottom reinforcement layers (Fig. 7a).

The maximum shear strain is observed in three zones of the model (Fig. 7b). The first zone starts at the bottom of the reinforced backfill (between the first and third strip level) and forms an angle of 30°. The second zone is a continuation of the first one in the retained backfill with a high angle (45°). Finally, the third zone is localised at the end of the strips, at the interface between the reinforced backfill and retained backfill.

3. Parametric study

The influence of several parameters (soil/strip interface parameters, strips parameters and reinforced soil parameters) on the behaviour of the MSE walls is studied. This study is based on the first modelling using reference parameters.
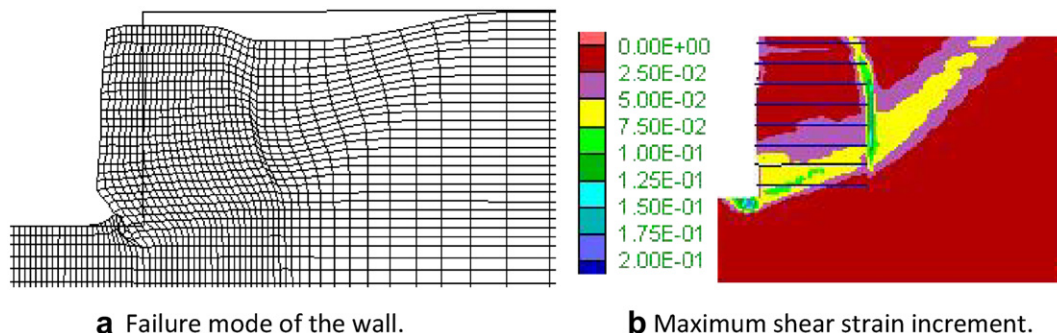

a Failure mode of the wall.　　**b** Maximum shear strain increment.

Fig. 7. Behaviour of the MSE Wall (6 m height) at ULS.

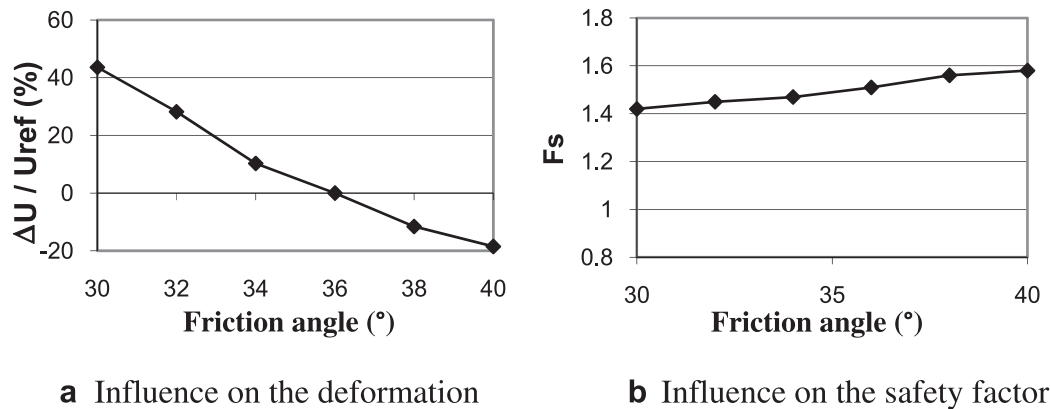**a** Influence on the deformation   **b** Influence on the safety factor

Fig. 8. Influence of the soil friction angle on the wall behaviour.

3.1. Influence of the soil parameters

The influence of the soil parameters is assessed by applying variations to the five parameters of the constitutive model. The results of the calculation show that the friction angle and the cohesion present a high influence on the deformation and on the safety factor of MSE Walls (Table 7). A decrease of 16% (36–30°) of the friction angle leads to a deformation increase of 45% and reduces the safety factor by 6% (Fig. 8a and b).

An increase of cohesion from 0 to 20 kPa decreases the deformation by 84% and increases the safety factor by 7%. For cohesion higher than 20 kPa, no more influence is observed (Fig. 9a and b).

3.2. Influence of the strip parameters

3.2.1. Strip type
The influence of the strip type is studied using the metallic strip and the new synthetic strip (GS HA) presented in Table 4.

The analysis of the results (Table 8) shows that the synthetic strips GS 50, which offer twice as much frictional width as the metallic strips per connection point (100 mm versus 50 mm), exhibit a higher safety level. The effect of the synthetic extensibility is compensated by a higher adherence capacity. However, the use of the new synthetic strips GS HA leads to a higher stability (+2.6% on Fs).

The displacements observed for the reinforced wall by synthetic strips GS 50 are 6 times higher than those observed in the case of metallic strips (−83% of deformation in the metallic strips case) and 1.1 time higher than those observed on strips GS HA (−6 % of deformation in the case of GS HA). These high displacements are observed in the horizontal and vertical directions. Reduction of

settlement in the reinforced soil by synthetic strips is lower compared to the results obtained with metallic reinforcements.

Concerning the failure mode, as in the case of strips GS 50, it can be described as sliding on the base, with the inference of the very bottom reinforcement levels.

3.2.2. Elastic modulus of the reinforcement
A virtual variation of the strip elastic modulus from 1.5 to 210 GPa has been studied, based on the cross-sectional geometry of the steel strips (i.e., 50 mm × 4 mm). The calculation results show that, between 1.5 and 10 GPa, this parameter presents an important influence on the wall deformation and small influence on the safety factor. Above 10 GPa, the modulus increase seems to have no influence on the calculation results (Fig. 10a and b). This threshold value can be converted into reinforcement axial stiffness per unit area facing: 3500 kN/m^2.

3.3. Influence of the constitutive models

To highlight the influence of the soil constitutive model in the numerical modelling, the Duncan–Chang and CJS2 soil constitutive models were used for different cases of reinforcement (GS 50, GS HA and metallic HA).

The parameters of these soil constitutive models were defined by calibration on triaxial tests carried out under confinement of 30 kPa, 60 kPa and 90 kPa (Tables 9 and 10).

3.3.1. Duncan & Chang Hyperbolic model (D&C)
The Duncan & Chang Hyperbolic constitutive model permits to take into account the nonlinearities of the soil before the failure. The
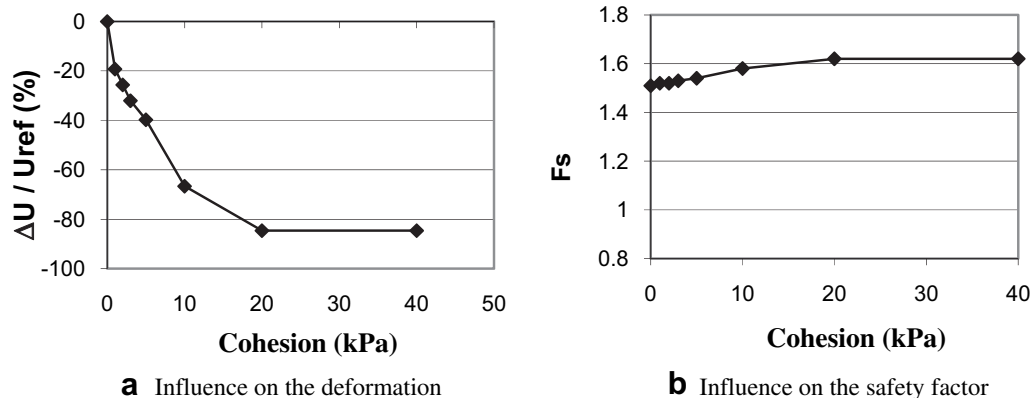

a Influence on the deformation   **b** Influence on the safety factor

Fig. 9. Influence of the cohesion on the wall behaviour.

Table 8
Comparison of the calculation results for the three strip types.

Strip	Fs	ΔFs/Fsr (%)	$|U|$ (mm)	U_x (mm)	U_y (mm)	$\Delta|U|/|U_r|$ (%)
GS 50	1.51	0	78	61	53	0
Metallic HA	1.48	−2	13.5	7.7	12	−83
GS HA	1.55	+2.6	73	57.8	49	−6

version used in the present study is able to model the very small strain and the nonlinear pre-failure soil behaviour. The nonlinear elastic part of the implemented model can be defined by stiffness parameters (Atkinson and Sallfors, 1991) and the degradation shape of these parameters. A slight alteration to the original model has been made and the plastic part of the model is defined by the Mohr–Coulomb failure criterion.

Stiffness parameters are given by the equations:

$$E_i = K_Y.P_a\left(\frac{P'}{P_a}\right)^{n_Y} \qquad (6)$$

$$K_i = K_B.P_a\left(\frac{P'}{P_a}\right)^{n_B} \qquad (7)$$

Which represent, respectively, initial values of the Young's modulus (Janbu, 1963) and Bulk's modulus (Duncan et al., 1980). K_Y and n_Y are the Young's modulus parameters; K_B and n_B are the Bulk's modulus parameters. P_a is the atmospheric pressure used for normalization of the stress input and P' is the average effective confining pressure.

Under small strain, the nonlinear shape is described by the hyperbolic relationship of Duncan and Chang (1970):

$$\sigma_1 - \sigma_3 = \frac{\varepsilon}{\dfrac{1}{E_i} + \dfrac{1}{(\sigma_1 - \sigma_3)_{ult}}} \qquad (8)$$

The stress–strain dependence is defined implicitly by the Failure Ratio (Rf coefficient) which represents the failure vicinity.

The values of the different parameters taken into account in the modelling are reported in Table 9.

3.3.2. CJS2 model

CJS2 model is an improved version of the CJS model developed by Cambou and Jafari (1987) for cohesionless soils. It is based on an elastic nonlinear part and two mechanisms of plasticity: a deviatoric mechanism and an isotropic mechanism. It allows to take into account the nonlinearity of the behaviour at low stress level and the

Table 9
Parameters of Duncan & Chang constitutive model.

Parameter	Value
Atmospheric pressure (kPa)	100
K_Y	500
n_Y	0.55
Failure Ratio	0.7
Cohesion (kPa)	0
K_B	600
n_B	0.5
Dilatancy angle (°)	6
Friction angle (°)	36

Table 10
Parameters of CJS2 constitutive model.

Parameter	Value
Shear modulus: G_0 (MPa)	20
Volumetric modulus: K_0 (MPa)	40
Material parameters: n	0.6
Dilatancy slope: β	0.176
Size of the characteristic surface: R_c	0.15
Deviatoric slope: A	0.0003
Size of the failure surface: R_m	0.3
Shape of the failure surface: γ	0.83
Plastic bulk modulus for the reference pressure Pa: K_0^p (MPa)	55

existence of dilatancy before the failure for dense or over-consolidated materials (Maleki et al., 2000). The use of this model requires the determination of two elastic parameters, five deviatoric mechanism parameters and one isotropic mechanism parameter (Table 10). The description of the model (Jenck et al., 2009) and its parameters are given in Appendix A.

3.3.3. Comparison between the different constitutive models
3.3.3.1. Case of standard synthetic straps GS 50. The numerical calculations show that the simulated wall behaviour using the three different constitutive models is slightly different (Fig. 11a–c). The maximum displacements observed at the wall face are located between the second and the third strip levels for MC, between the third and the fifth strip levels for D&C and CJS2. The CJS2 (more complex model) leads to a highest deformation area. So it seems necessary to correctly model the soil nonlinearity to better model the wall deformation.

The analysis of the soil/strip shear displacements confirms the slight difference between the results of the three models (Fig. 12a). The maximum shear displacement is underestimated by the MC
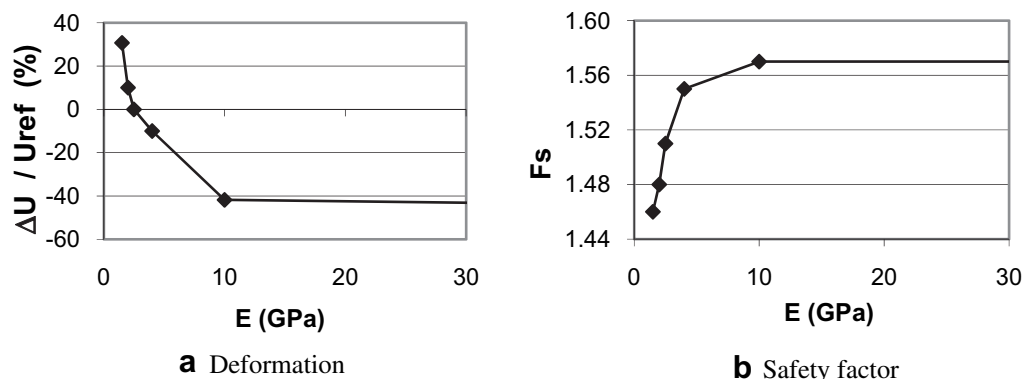

a Deformation   **b** Safety factor

Fig. 10. Influence of the strip elastic modulus on the wall behaviour.

Fig. 11. Comparison of horizontal displacements for the three soil constitutive models (reference case).

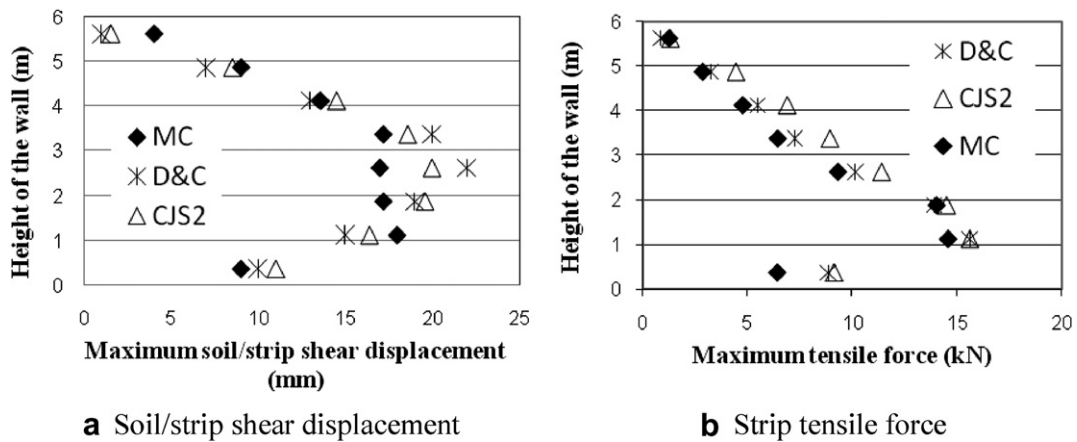**a** Soil/strip shear displacement **b** Strip tensile force

Fig. 12. Comparison of the results of the three soil constitutive models (reference case).

constitutive model (15% less than with CJS2 at the fourth strip). The D&C contitutive model overestimates the maximum shear displacement (10% more than with CJS2 at the fourth strip). So, the nonlinear models lead to a highest shear displacement. On the other hand, the fact that CJS2 take into account the existence of

dilatancy before the failure reduces the shear displacement compared to D&C.

The maximum tensile forces on the strips (Fig. 12b) are observed between the second and the third strip levels for the three models. The maximum tensile force value (second and
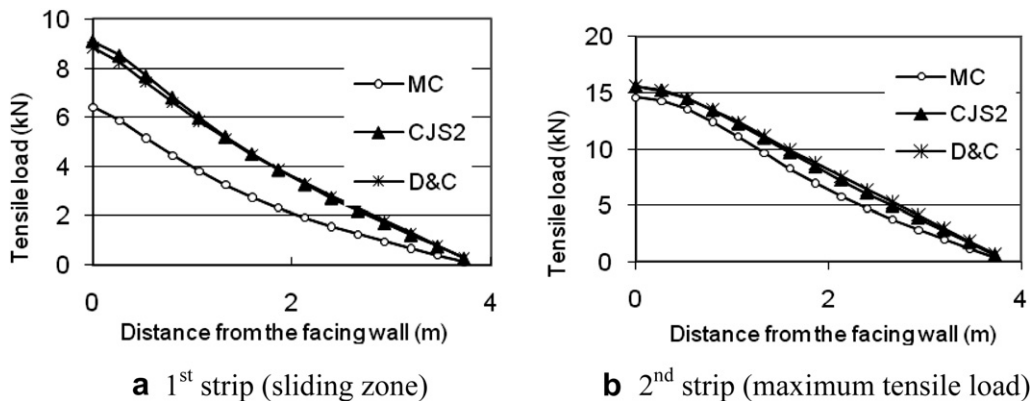

a 1st strip (sliding zone) **b** 2nd strip (maximum tensile load)

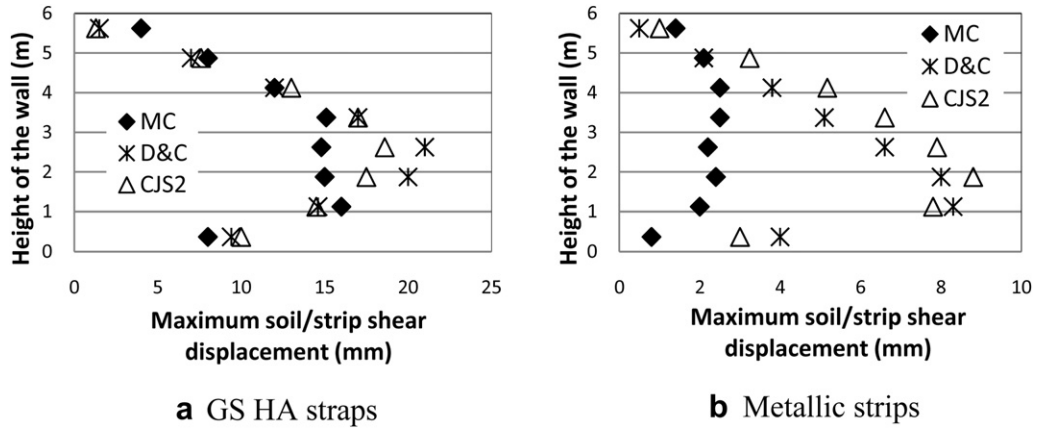**Fig. 13.** Tensile loads along the strips (reference case).

Fig. 14. Comparison of the maximum soil/strip shear displacement for three soil constitutive models.
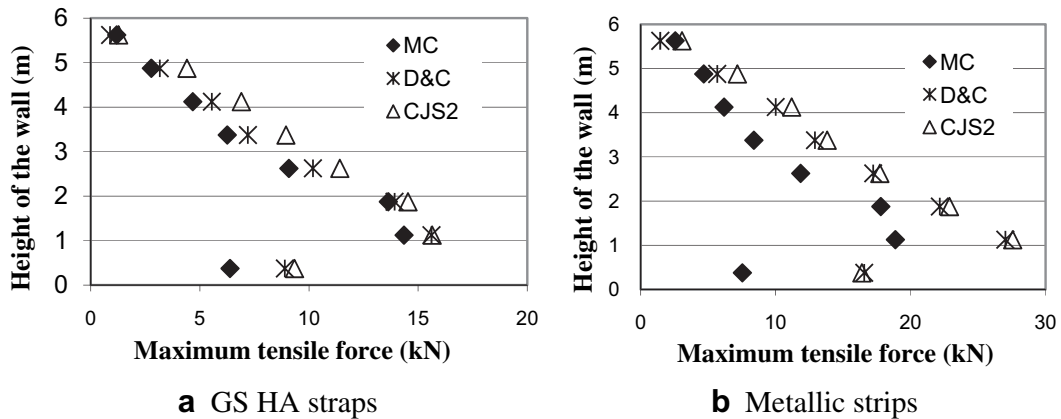

Fig. 15. Comparison of the maximum tensile force for three soil constitutive models.

third strips) for the D&C model is in good agreement with the CJS2 value. However, for the other levels (at top part of the wall), it seems that the MC and the D&C constitutive models underestimate the tensile loads. So, considering the existence of dilatancy before the failure by CJS2 model leads to higher tensile loads on the strips at the top part of the wall. These results seem to be more realistic knowing that the dilatancy is important under low stresses.

Fig. 13 shows that the MC model underestimate the tensile loads along the strips in two important zones: at the 1st strip level (up to −30%) and at 2nd strip (up to −6%). So, at least a nonlinear soil constitutive model (as D&C) is necessary to correctly model the tensile loads on the strips at the important zones of the wall.

3.3.3.2. Case of new synthetic straps GS HA and metallic strips. The calculations carried out on the GS HA straps and metallic strips
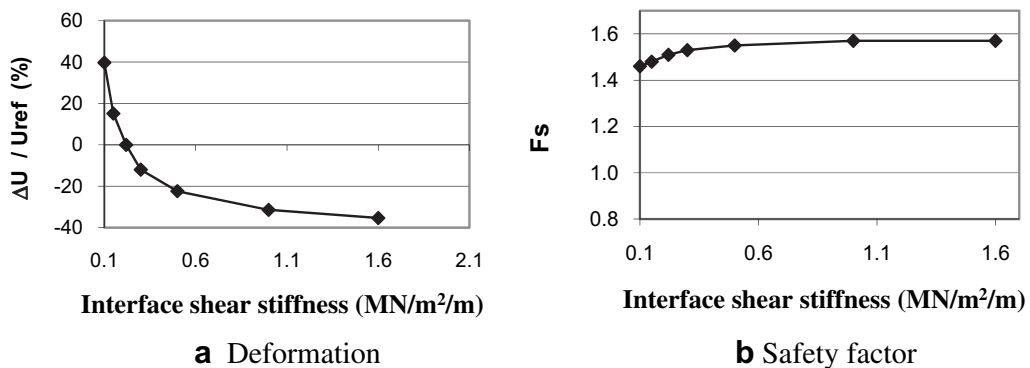

Fig. 16. Influence of the interface shear stiffness on the wall behaviour.

Table 11
Results of calculation with and without simulation of compaction.

Strip	Fs	$|\Delta Fs|/Fsr$ (%)	$|U|$ (mm)	$|U_x|$ (mm)	$|U_y|$ (mm)	$|\Delta U|/$ $|U_r|$ (%)
GS 50 without compaction	1.51	–	78	61	53	–
GS 50 compaction 8 kPa	1.51	0	96	71	66	23
GS 50 compaction 10 kPa	1.51	0	100	73	70	30
GS 50 compaction 16 kPa	1.53	1.3	118	86	85	51

parametric study shows that the influence of this parameter is important for the safety factor but very low for the deformation. The maximum calculated variation from the reference value is 7% for the safety factor and 2% for the deformation. However, the interface shear stiffness (k_b) variations lead to an important variation of the wall deformation. The deformation increases by factor of 2 for a reduction of the interface shear stiffness from 1.6 to 0.1 MN/m²/m. For the safety factor, the influence is less important (4%) (Fig. 16).

a Soil/reinforcement shear displacement   **b** Maximum tensile force on the straps
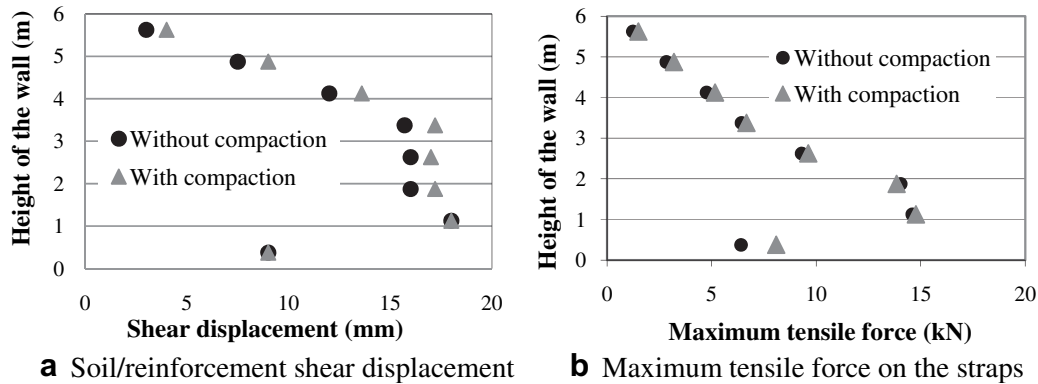
Fig. 17. Effect of the compaction (vertical stress of 10 kPa).

confirm the results obtained in the case of GS 50 straps. They show that the use of three different constitutive soil models leads to differences. The maximum shear displacement is underestimated by the MC soil constitutive model in the cases of GS HA straps and Metallic strips (Fig. 14). This underestimation is more important in the case of the metallic strips (up to 70%).

Concerning the tensile force on the strips (Fig. 15), the CJS2 model leads to higher values compared to D&C and MC models. The MC model gives the lower values especially in the case of metallic strips (up to −30%). These results confirm that a nonlinear soil constitutive model (as D&C) is necessary to correctly model the shear displacement and the tensile loads on the strips. The maximum difference obtained between CJS2 and D&C is equal to 22%.

The analysis of the tensile forces on the strips in the important zones of the wall and the shear displacement at the soil/reinforcement interfaces, show that contrary to the conclusions deduced by Huang et al. (2009) and Ling and Liu (2009), the use of models with different level of complexity, leads to different results.

3.4. Influence of the soil/reinforcement interface parameters

The interface friction coefficient f^*_0 and f^*_1 were, respectively, varied between 3–0.6 and 0.6–0.3 in the reference model. This

The experimental pullout tests results showed that the interface parameters vary versus the confinement stresses. A modelling of the MSE Wall was made using the interface shear stiffness values (k_b) which varies from the top to the bottom of the wall in order to highlight the influence of this variation. The value of this parameter (pullout test results) at each strip level is, from top to bottom:

- 1st and 2nd strips level: $k_b = 0.6$ MN/m²/m;
- 3rd and 4th strips level: $k_b = 0.4$ MN/m²/m;
- 5th and 6th strip level: $k_b = 0.2$ MN/m²/m;
- 7th and 8th strip level: $k_b = 0.15$ MN/m²/m.

The results show that taking into account the evolution of the shear stiffness versus the confinement, presents an influence on the deformation of the wall (+15%) but almost no influence on the stability of the wall (<+1%).

3.5. Influence of the soil compaction

To study the influence of the compaction in the numerical simulations, we have adopted the process defined by Hatami and Bathurst (2006). These authors consider this effect as a vertical stress applied at the top of the soil. Comparing between predicted
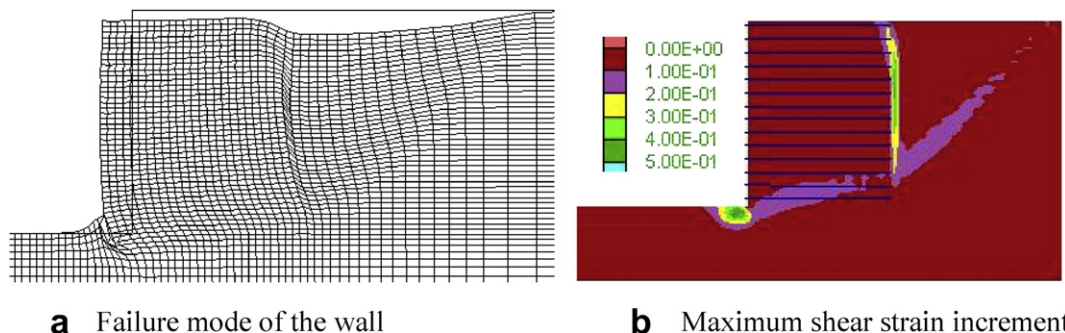

a Failure mode of the wall   **b** Maximum shear strain increment

Fig. 18. Behaviour of the MSE Wall (10.5 m height) at ULS.

Table 12
Definition of four categories of influence.

Variation of Fs%	Variation of U%	Symbol
0–5	0–10	–
5–10	10–25	+
10–20	25–50	++
>20	>50	+++

and measured wall response (for two types of sand), they have determined that the value of the vertical stress is equal to 8 kPa (respectively, 16 kPa) for sand with a Young's modulus of 40 MPa (respectively, 80 MPa).

In our case, the sand has a Young's modulus of 50 MPa, by linear interpolation a vertical stress of 10 kPa has been deduced.

To study the influence of the compaction, three different calculations have been performed by introducing a stress load on each soil layer at its set up. The loads simulated in the first, second and third calculations are, respectively, 8 kPa, 10 kPa and 16 kPa. In this numerical modelling, the stress load is removed immediately after the introduction of the next layer in all stages of construction.

The modelling results show that the displacements calculated on the MSE wall in the reference case are more important when the compaction is simulated (Table 11). An increase of 23%, 30% and 51% are, respectively, measured for stress loads of 8 kPa, 10 kPa and 16 kPa. Concerning the stability of the wall, the safety factor Fs increased slightly (+1.3%) for a load of 16 kPa but does not change for loads of 8 kPa and 10 kPa. The deformation difference shows that it is necessary to estimate with accuracy the loading stress in order to simulate the compaction.

The analysis of the shear displacement between the soil and reinforcement shows a slight difference in results between the calculation taking into account a loading stress of 10 kPa and the calculation performed without simulation of compaction (Fig. 17a). The maximum shear displacement between the soil and rein-forcement are slightly overestimated by the calculation that does not take into account the compaction (about 10% in most of rein-forcement levels). Concerning the tensile force on the straps (Fig. 17b), they are slightly underestimated by the calculation when the soil compaction is not taken into account (about −2% in most reinforcement levels).

These results infer that soil compaction needs to be taken into account in numerical modelling in order to estimate with accuracy the deformation of the structure. However, it is difficult to define with accuracy the value of the equivalent loading stress allowing to simulate the real compaction in the calculations. A bad esti-mation of this stress can induce an overestimation of the wall deformation. This approximate way to take into account the effects of compaction is questionable because it is not able to simulate all the effects of compaction (density change, partial tension of reinforcement).

Table 13
Parameters influence on the wall behaviour.

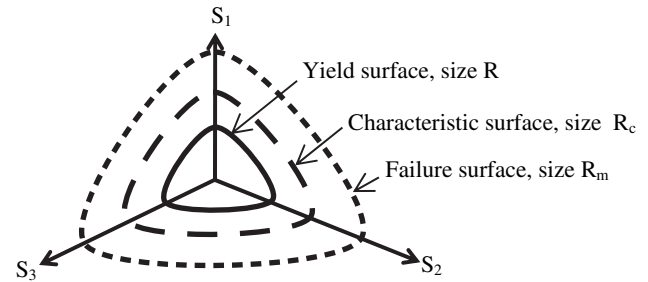| Parameter		Degree of influence	
		ULS	SLS
Interface	Interface shear stiffness	–	++
	Friction coefficient	+	–
Strip	Strip elastic modulus	–	+++
Soil	Young modulus	–	–
	Poisson's ratio	–	–
	Friction	+	++
	Cohesion	+	+++
	Dilatancy	–	+

Fig. 19. Deviatoric mechanism of the CJS2 model in the deviatoric stress (S1, S2, S3) plane.

3.6. Influence of the wall height

To study the influence of the wall height, a model of 10.5 m height was simulated. It is made of 7 superimposed panels and reinforced by 14 levels of 8 m long reinforcements. The reference parameters are used in this numerical model.

The failure analysis shows that the behaviour of the 10.5 m high wall is the same as that for the 6 m high wall. It occurs by sliding of the unstable ground zone (Fig. 18a). The maximum shear strain is observed in three zones as in the reference case (Fig. 18b).

3.7. Influencing parameters

A scale has been made to present the influence of each parameter. Two results are presented: the safety factor and the wall deformation. For each of the parameter the scale is divided in four categories and each category is defined by a symbol (see Table 12).

Table 13 analysis allows to define the parameters that influence the wall behaviour. Concerning the safety, the soil friction angle, the soil cohesion and the interface friction coefficient present the most important influence.

For the wall deformation, the soil cohesion and the strip elastic modulus are the most important influencing parameters. The interface shear stiffness, the soil friction and the dilatancy angle present a significant influence but that is low compared to the strip elastic modulus and the soil cohesion.

4. Conclusions

The results of this numerical study allowed to deduce in one hand, interesting conclusions concerning the behaviour of the MSE structures, and in the other hand, to highlight the importance of each parameter in the numerical modelling. The importance of this study lies in the fact that the method and the parameters taken into account in the modelling are as realistic as possible. Indeed, the construction stages are reproduced as in actual conditions, the reference parameters of the synthetic strips were validated by calibration on pullout tests and nonlinear constitutive models validated on triaxial test are used to reproduce with accuracy the soil behaviour.

The first modelling carried out using reference parameters allows to draw two important results:

- The synthetic strips parameters lead to high horizontal displacements of the facing wall in the numerical calculation.
- The ULS analysis shows that failure occurs by sliding of MSE blocks, accompanied with adherence rupture of the bottom reinforcement layers. Maximum shear strain shows that the unstable part is localised on a slightly inclined plane at the-bottom of the reinforced block. This plane is prolonged into

the retained backfill by another plane with a higher inclination. Another shearing plane is localised at the interface between the reinforced backfill and retained backfill.

The parametric study allows to define the parameters that influence the wall behaviour and the importance of each parameter. The conclusions deduced from this study are:

- The soil shear strength parameters present the higher influence on the stability and the deformation of the MSE Walls.
- It seems necessary, at least, to use a nonlinear soil constitutive model (as D&C) to correctly model the wall deformation and the tensile loads on the strips, especially in the case of large strains. If experimental data is sufficient, using a model which take into account the existence of dilatancy before the failure (as CJS2) allow to better estimate the shear displacement and the tensile loads on the strips.
- The use of synthetic strips two times larger than metallic strips leads to higher wall stability and increases the adherence capacity. This stability is even higher using the newly developed High Adherence synthetic strips. Concerning the failure modes, they are similar for the three strip types.
- The parametric study on the strip elastic modulus shows that this parameter presents an important influence on the stability and the wall deformation for axial stiffness values lower than 3500 kN/m^2 of wall face.
- The study of the interface parameters shows that the variations of the interface shear stiffness leads to an important variation of the wall deformation. A good estimation of this parameter (e.g., by laboratory pullout test) for each reinforcement type seems to be essential for proper assessment of the structure displacements.

Appendix A

CJS2 model is based on an elastic nonlinear part and two mechanisms of plasticity: a déviatoric mechanism and an isotropic mechanism:

The elastic part is given by the shear and the bulk modulus G and K.

$$G = G_0 \cdot \left[\frac{I_1}{3 \cdot P_a} \right]^n \tag{9}$$

$$K = K_0 \cdot \left[\frac{I_1}{3 \cdot P_a} \right]^n \tag{10}$$

Where G_0, K_0 and n are material parameters for the reference pressure Pa (usually 100 kPa). I_1 is the first stress invariant.

The deviatoric mechanism (for deviatoric stresses) is described by three surfaces in the deviatoric stress space (Fig. 19).

The expression of the yield function of the deviatoric mechanism (f^d) is given by Eq. (11), where s_{II} is the deviatoric stress tensor second invariant and h is a function of the Lode angle θ (γ is a model parameter). The size of the surface R varies during the loading according to isotropic hardening:

$$f^d = s_{II} \cdot h(\theta) - R \cdot I_1, \quad \text{with } s_{II} = \sqrt{s_{ij}s_{ij}} \text{ and } h(\theta)$$

$$= \left(1 - \gamma \cdot \sqrt{54} \cdot \frac{\det s_{ij}}{s_{II}^3} \right)^{1/6} \tag{11}$$

Failure occurs when the deviatoric stress state reaches the failure surface (Equation (12)), R_m is a model parameter,

corresponding to the size of the failure surface and related to the friction angle:

$$f^R = s_{II} \cdot h(\theta) - R_m \cdot I_1 \tag{12}$$

The characteristic state is taken into account, which makes it possible to simulate dilatancy before failure for dense materials. The characteristic surface is given by Equation (13), R_c is a model parameter:

$$f^c = s_{II} \cdot h(\theta) - R_c \cdot I_1 \tag{13}$$

The isotropic hardening of the deviatoric mechanism involves the model parameters R_m, R_c and an additional parameter A (Cambou and Jafari, 1987).

The isotropic mechanism yield surface is a plane perpendicular to the hydrostatic axis in the principal stress space (Equation (14), Q being the hardening variable, determined by the isotropic hardening mechanism, Cambou and Jafari, 1987). Isotropic hardening of this mechanism is governed by the model parameter K_0^p (the plastic bulk modulus for the reference pressure Pa).

$$f^i = \frac{I_1}{3} - Q \tag{14}$$

References

AASHTO, 2002. Standard specifications for highway bridges, Seventeenth ed., Washington, D. C.

Abdelouhab, A., Dias, D., Freitag, N., 2009. Physical and analytical modelling of geosynthetic strip pullout behaviour. Geotextiles and Geomembranes 28 (1), 44–53.

Al Hattamleh, O., Muhunthan, B., 2006. Numerical procedures for deformation calculations in the reinforced soil walls. Geotextiles and Geomembranes 24 (1), 52–57.

Allen, T.M., Bathurst, R.J., Berg, R.R., 2002. Global level of safety and performance of geosynthetic walls: a historical perspective. Geosynthetics International 9 (5–6), 395–450.

Atkinson J.H., Sallfors G., 1991. Experimental determination of stress–strain–time characteristics in laboratory and in situ tests. In: Proceedings of the 10th European Conference on Soil Mechanics and Foundation Engineering, Florence, vol. 3, pp. 915–956.

Anon., 2009. Nf P 94-270: Renforcement des Sols. Ouvrages en Sol Rapporté Renforcé Par Armatures ou Nappes Extensibles et Souples. Dimensionnement. Editions AFNOR.

Anon, 1998. Nf P 94-220: Renforcement des Sols. Ouvrages en Sol Rapporté Renforcé Par Armatures ou Nappes Peu Extensibles et Souples. Dimensionnement. Editions AFNOR.

Bathurst, R.J., Allen, T.M., Walters, D.L., 2005. Reinforcement loads in geosynthetic walls and the case for a new working stress design method. Geotextiles and Geomembranes 23 (4), 287–322.

Bergado, D.T., Teerawattanasuk, C., 2008. 2D and 3D numerical simulations of reinforced embankments on soft ground. Geotextiles and Geomembranes 26, 39–55.

Cambou, B., Jafari, K., 1987. A constitutive model for granular materials based on two plasticity mechanisms. In: Saada, A.S. (Ed.), Constitutive Equations for Granular Non-Cohesive Soils. Balkema, Rotterdam, pp. 149–167.

Duncan, J.M., Chang, C.Y., 1970. Nonlinear analysis of stress and strain in soils. Journal of the Soil Mechanics and Foundations Division, ASCE 96 (SM5), 1629–1653.

Duncan, J.M., Byrne, P., Wong, K.S., Mabry, P., 1980. Strength, Stress–Strain and Bulk Modulus Parameters for Finite Element Analysis of Stress and Movements in Soil Masses. UCB/GT/80-01. College of California, Berkeley, California.

Elias, V., Christopher, B., Berg, R.R., 2001. Mechanically Stabilized Earth Walls and Reinforced Soil Slopes Design and Construction Guidelines. FHWA-NHI-00-043. Federal Highway Administration, Washington, D. C.

Flavigny, E., Desrues, J., Palayer, B., 1990. Le sable d'Hostun RF. Note technique. Revue Française de Géotechnique 53, 67–70.

Gay, O., 2000. Modélisation physique et numérique de l'action d'un glissement lent sur des fondations d'ouvrages d'art. Thèse de doctorat en Mécanique, Laboratoire 3S, Grenoble 1.

Hatami, K., Bathurst, R.J., 2006. Parametric analysis of reinforced soil walls with different backfill material properties. In: NAGS' 2006 Conference, Las Vegas, Nevada, USA, pp. 1–15.

Ho, S.K., Rowe, R.K., 1994. Prediction behavior of two centrifugal model soil walls. Journal of Geotechnical Engineering, ASCE 120 (10), 1845–1873.

Huang, B., Bathurst, R.J., Hatami, K., 2009. Numerical study of reinforced soil segmental walls using three different constitutive soil models. Journal of Geotechnical and Geoenvironmental Engineering, ASCE 135 (10), 1486–1498.

Itasca Consulting Group. FLAC2D. User's guide. 2006.

Janbu, N., 1963. Soil compressibility as determined by oedometer and triaxial tests. In: Proceedings of the 3rd European Conference on Soil Mechanics and Foundation Engineering, vol. 1, Wiesbaden, Germany. pp. 19—24.

Jenck, O., Dias, D., Kastner, R., 2009. Three-dimensional numerical modeling of a piled embankment. International Journal Of Geomechanics, ASCE 9, 102.

Khedkar, M.S., Mandal, J.N., 2009. Pullout behaviour of cellular reinforcements. Geotextiles and Geomembranes 27, 262—271.

Koerner, R.M., Soong, T.Y., 2001. Geosynthetic reinforced segmental retaining walls. Geotextiles and Geomembranes 19 (6), 359—386.

Leshchinsky, D., 2009. On global equilibrium in design of geosynthetic reinforced walls. Journal of Geotechnical and Geoenvironmental Engineering 135, 309.

Ling, H.I., Liu, H., Mohri, Y., 2005. Parametric studies on the behavior of reinforced soil retaining walls under earthquake loading. Journal of Engineering Mechanics 131, 1056.

Ling, H.I., Liu, H., 2009. Deformation analysis of reinforced soil retaining walls — simplistic versus sophisticated finite element analyses. Acta Geotechnica 4, 203—213.

Maleki, M., Dubujet, P., Cambou, B., 2000. Modélisation hiérarchisée du comportement des sols. Revue Française de Génie Civil 4 (No. 7—8), 895—928.

Park, T., Tan, S.A., 2005. Enhanced performance of reinforced soil walls by the inclusion of short fiber. Geotextiles and Geomembranes 23 (4), 348—361.

Quang, T.S., Hassen, G., De Buhan, P., 2008. Modélisation multiphasique appliquée à l'analyse de stabilité d'ouvrage en sols renforcés avec prise en compte d'une condition d'adhérence sol-armatures. Studia Geotechnica et Mechanica XXX (No. 1—2).

Schlosser, F., Elias, V., 1978. Friction in Reinforced Earth, A.S.C.E. Convention, Pittsburgh, April 24—28.

Sieira, A.C.C.F., Gerscovich, D.M.S., Sayão, A.S.F.J., 2009. Displacement and load transfer mechanisms of geogrids under pullout condition. Geotextiles and Geomembranes 27 (4), 241—253.

Skinner, G.D., Rowe, R.K., 2005. Design and behaviour of a geosynthetic reinforced retaining wall and bridge abutment on a yielding foundation. Geotextiles and Geomembranes 23 (3), 235—260.

Su, L.J., Chan, T.C.F., Yin, J.H., Shiu, Y.K., Chiu, S.L., 2008. Influence of overburden pressure on soil—nail pullout: resistance in a compacted fill. Journal of Geotechnical and Geoenvironmental Engineering 134, 1339.

Won, M.S., Kim, Y.S., 2007. Internal deformation behavior of geosynthetic-reinforced soil walls. Geotextiles and Geomembranes 25 (1), 10—22.

Yoo, C., Jung, H.Y., 2006. Case history of geosynthetic reinforced segmental retaining wall failure. Journal of Geotechnical and Geoenvironmental Engineering 132, 1538.

Yoo, C., Kim, S.B., 2008. Performance of a two-tier geosynthetic reinforced segmental retaining wall under a surcharge load: full-scale load test and 3D finite element analysis. Geotextiles and Geomembranes 26 (6), 460—472.